ELSEVIER

Contents lists available at ScienceDirect

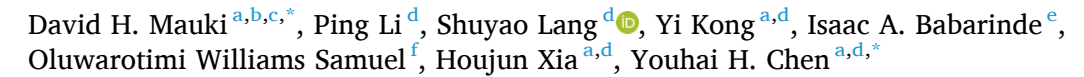
Computational and Structural Biotechnology Reports

journal homepage: www.sciencedirect.com/journal/csbr



Research article

Unveiling *TNFAIP8L2*-related immune evasion mechanisms in colorectal cancer



- a Key Laboratory for Cellular and Gene Therapy of Guangdong, Faculty of Pharmaceutical Sciences, Shenzhen University of Advanced Technology, Shenzhen, China
- ^b Department of Neurosurgery, West China Hospital, Sichuan University, Chengdu, China
- ^c Institute of Neurological Disease, National-Local Joint Engineering Research Center of Translational Medicine, West China Hospital, Sichuan University, Chengdu 610041. China
- d Center for Cancer Immunology, Shenzhen Institute of Advanced Technology, Chinese Academy of Sciences, Shenzhen, China
- ^e Laboratory of Inflammation and Vaccines, Institute of Biomedicine and Biotechnology, Shenzhen Institute of Advanced Technology, Chinese Academy of Science, Shenzhen
- f School of Computing and Engineering, University of Derby, Derby DE22 3AW, United Kingdom

ARTICLE INFO

Keywords: Bioinformatics Colon/Colorectal cancer Immune evasion TNFAIP8L2/TIPE2 Tumor immunity/immunotherapy

ABSTRACT

Colorectal cancer (CRC) remains to be a leading cause of cancer-related mortality worldwide. Although immune evasion appears to play a critical role in CRC progression, the underlying mechanisms are poorly defined, necessitating further scientific investigation. Here we report a differential co-expression gene pattern involving TNFAIP8L2 (TIPE2), a newly described immune checkpoint gene, which may be employed by CRC to evade immune surveillance. Single-cell RNA sequencing and bioinformatic analyses of CRC revealed significant positive correlations between TNFAIP8L2 and the metastatic gene OLR1 as well as the immune checkpoint gene PDL1, indicating potential functional synergistic interactions among these genes. Additionally, the TNFAIP8L2 differentially co-expressed genes (Dco-EGs) in macrophages were positively associated with the p53 signaling pathway, indicating an important mechanism in regulating tumor immunity in CRC. These findings provide new insights into the complex mechanism of immune evasion in CRC, laying the foundation for the development of innovative tumor immunotherapies.

1. Introduction

Colorectal cancer (CRC) continues to be one of the most common and lethal cancers globally, contributing substantially to cancer-related morbidity and mortality. It is the third most frequently diagnosed cancer and the fourth leading cause of cancer death worldwide, with an estimated 1.2 million new cases and 600,000 deaths each year [1–3]. Despite advances in early detection and treatment, the prognosis for patients with advanced CRC remains poor, largely due to the complex mechanisms underlying tumor progression and immune evasion [1, 4–6]. The tumor microenvironment (TME) plays a pivotal role in shaping the malignant characteristics of cancer, including immune evasion, which allows cancer cells to escape immune surveillance [4,7]. Understanding the molecular mechanisms that drive immune evasion in

CRC is therefore critical for developing effective therapeutic strategies.

Immune evasion in colorectal cancer (CRC) is mediated by multiple mechanisms, including the upregulation of immune checkpoint molecules such as programmed cell death ligand 1 (PD-L1) and cytotoxic T-lymphocyte-associated protein 4 (*CTLA4*) [8,9]. These molecules inhibit anti-tumor immunity by engaging with their respective receptors on immune cells, leading to T-cell exhaustion and immune suppression [10–13]. The development of immune checkpoint inhibitors (ICIs) such as pembrolizumab targeting PD-1/PD-L1 and Ipilimumab targeting *CTLA4* has revolutionized cancer treatment, demonstrating remarkable clinical success across multiple malignancies [14–16]. However, the efficacy of ICIs in CRC has been strikingly limited, particularly in microsatellite-stable (MSS) tumors, which constitute the majority of CRC cases [17,18]. This therapeutic resistance highlights the urgent

E-mail addresses: davidHmauki@outlook.com (D.H. Mauki), yh.chen@siat.ac.cn (Y.H. Chen).

https://doi.org/10.1016/j.csbr.2025.100041

Received 10 September 2024; Received in revised form 10 April 2025; Accepted 11 April 2025 Available online 12 April 2025

2950-3639/© 2025 The Author(s). Published by Elsevier B.V. on behalf of Research Networks AS. This is an open access article under the CC BY license (http://creativecommons.org/licenses/by/4.0/).



^{*} Corresponding authors at: Key Laboratory for Cellular and Gene Therapy of Guangdong, Faculty of Pharmaceutical Sciences, Shenzhen University of Advanced Technology, Shenzhen, China.

need to identify novel immune checkpoint molecules and their associated pathways that could serve as targets for combination therapies.

In this study, we focus on TNFAIP8L2 (Tumor Necrosis Factor Alpha-Induced Protein 8 Like-2), a member of the TNFAIP8 family, which has recently emerged as a potential immune checkpoint gene with dual roles in immune regulation and cancer progression [19-21]. Also known as TIPE2, TNFAIP8L2 is an important negative regulator of innate and adaptive immunity through the inhibition of TLR and TCR signaling in order to maintain immune homeostasis both in inflammation and carcinogenesis [19,22]. It is also involved in modulating cellular polarization and chemotaxis [19,23]. TNFAIP8L2 has been shown to exhibit distinct, tissue-specific roles in cancer progression. In hepatocellular carcinoma (HCC), TNFAIP8L2 suppresses tumor growth and metastasis by inhibiting the PI3K/AKT signaling pathway [24]. By contrast, in CRC, TNFAIP8L2 exhibits context-dependent duality: TNFAIP8L2 tumor initiation promotes murine during AOM/DSS-induced inflammatory carcinogenesis, while its overexpression suppresses tumor cell proliferation and survival in established murine CRC models [22]. The roles of human TNFAIP8L2 in CRC remain to be established.

To address this knowledge gap, we employed a multi-omics approach, integrating scRNA-seq and bulk RNA sequencing data from CRC patients, to explore the role of human TNFAIP8L2 in shaping the immune landscape of CRC. Our analysis revealed that TNFAIP8L2 is highly expressed in myeloid cell populations, particularly conventional or tumor-associated macrophages (TAMs), cycling macrophages, and dendritic cells. Furthermore, we identified distinct co-expression patterns of TNFAIP8L2 together with key immune regulators, including OLR1 (Oxidized Low-Density Lipoprotein Receptor 1), and ZG16 (Zymogen Granule Protein 16). OLR1, a gene linked to metastasis and poor prognosis [25], was positively correlated with TNFAIP8L2, while ZG16, an anti-tumor gene [26], exhibited an inverse relationship with TNFAIP8L2. Notably, TNFAIP8L2 was positively correlated with the immune checkpoint PD-L1, suggesting a potential TNFAIP8L2-mediated mechanism for immune escape. Functional enrichment analysis of TNFAIP8L2 co-expressed genes revealed their involvement in critical pathways such as p53 signaling, leukocyte chemotaxis, and cytokine signaling, all of which are known to play important roles in immune regulation and tumor progression [27-29]. Additionally, we observed a positive correlation between TNFAIP8L2 and regulatory T cell (Treg) markers, such as FOXP3 and CTLA4, suggesting a potential cooperative role in mediating immunosuppression within the CRC TME [30]. These findings position TNFAIP8L2 as a central player in CRC immune evasion and highlight its potential as a therapeutic target, particularly in combination with existing immune checkpoint inhibitors.

Our study provides novel insights into the role of *TNFAIP8L2* in CRC immune evasion and identifies the *TNFAIP8L2-OLR1-PD-L1* axis as a promising target for combinatorial immunotherapy. By leveraging computational biology and multi-omics data, we unravel the complex interplay between *TNFAIP8L2* and its co-expressed genes, offering a roadmap for the development of precision therapeutic strategies for CRC.

2. Results

2.1. Single-cell transcriptome analyses of human colon cancer revealed new dynamics of TME

The tumor microenvironment (TME) plays a pivotal role in shaping the malignant characteristics of cancers [7]. Factors such as expression of PD-L1 are crucial in developing resistance to immunotherapy [12,13]. Understanding the factors influencing PD-L1 expression in the TME is important for enhancing the efficacy of immunotherapies and improving patient outcomes through personalized treatment strategies [31].

In this study, we analyzed publicly available scRNA-seq datasets from 62 CRC patients, including their tumor and adjacent non-tumorous

tissues (Fig. 1A). The dataset, comprising 370,114 cells and 31,873 genes, was processed using R software v4.3.3 to segregate cells into 24 distinct clusters based on their transcript profiles, and visualized using uniform manifold approximation (UMAP) (Fig. S1A). To address potential redundancy in the dataset of 31,873 genes, we focused on highly variable genes and used PCA to reduce dimensionality. This approach minimized the impact of redundant genes with overlapping expression patterns, ensuring that the clustering results reflected biologically meaningful cell populations. By cross-referencing known cell class-specific marker genes (Fig. S1B) [32], we identified three major cell classes: epithelial, immune, and stromal (Fig. 1B). Notably, a higher proportion of cells infiltrated tumor tissues compared to normal tissues (Fig. 1C), with immune cell lineages showing the most significant enrichment (Fig. S2).

Further subclassification of immune cells revealed 15 major subclusters (Fig. S1C), representing various immune cell types (Fig. 1D) based on canonical markers (Fig. S1D). These included NK/T cells, Tregs, neutrophils, dendritic cells, B cells, monocytes, macrophages, plasma cells, and mast cells. During colon tumorigenesis, we observed increased infiltration of both lymphoid and myeloid cell types in tumor tissues compared to normal tissues with the exceptional of B cells (Fig. 1E-F).

2.2. Identification of TNFAIP8L2 co-expressed genes in human colon cancer

TNFAIP8L2 is a newly identified immune checkpoint gene that regulates cancer progression [19,20]. To identify potential TNFAIP8L2 co-expression patterns in CRC, we first clustered myeloid cells based on canonical markers (Fig. S1F). Eight distinct subclusters (Fig. S1E) including macrophages (cluster 0, C0), monocytes (C1), conventional dendritic cells (cDCs, C2), neutrophils (C3), cycling macrophages (C4), mature regulatory DCs (mregDCs, C5), plasmacytoid DCs (pDCs, C6), and mast cells (C7) (Fig. 2A-B) were identified. Notably, we found that the proportion of myeloid cells in tumor tissues was significantly higher than in normal tissues (Fig. 2B-C) with macrophages and monocytes showing the most pronounced differences (Fig. 2D). TNFAIP8L2 was significantly expressed in conventional or tumor-associated macrophages, conventional dendritic cells (cDCs), and cycling macrophages (Fig. 3A). Its expression levels differed significantly between normal and tumor tissues, particularly in macrophages (Fig. 3B).

To understand the relationship between *TNFAIP8L2* and other genes in the TME, we performed correlation analyses to identify *TNFAIP8L2* co-expressed genes (co-EGs) (see Methods for more details). Cells that expressed *TNFAIP8L2* gene were designated as Group 1 and cells that did not as Group 2 (Fig. 3C-D). Co-expressed genes in Group 1 were referred to as *TNFAIP8L2* co-Egs.

2.3. Enrichment analysis of TNFAIP8L2 single-cell co-expressed transcriptomes revealed its connection with OLR1, PD1, and p53

Differential analysis of Group 1 cells identified a total of 12,801 Dco-EGs (Supplementary Table S1), with 8376 and 1, 366 genes showing significant changes based on p-value < 0.05, and adjusted p-value < 0.05, respectively. To minimize false positives, we used the adjusted p-value for downstream analyses. Of note, TNFAIP8L2 was significantly downregulated in tumor tissues based on the unadjusted p-value < 0.05 (log fold change = -0.7455, p-value = 1.36E-05, MAST statistical test), but this significance was not retained after adjusting for multiple testing (log fold change = -0.7455, p-value = 0.4344, MAST statistical test) (Fig. 3D).

Of the 1366 significant Dco-EGs (adjusted p-value < 0.05) (Supplementary Table S2), 130 genes were downregulated (absolute log fold change < 0.5) (Supplementary Table S3), and 611 genes were upregulated (absolute log fold change > 0.5) (Supplementary Table S4). Although *TNFAIP8L2* was downregulated in the TME, this does not

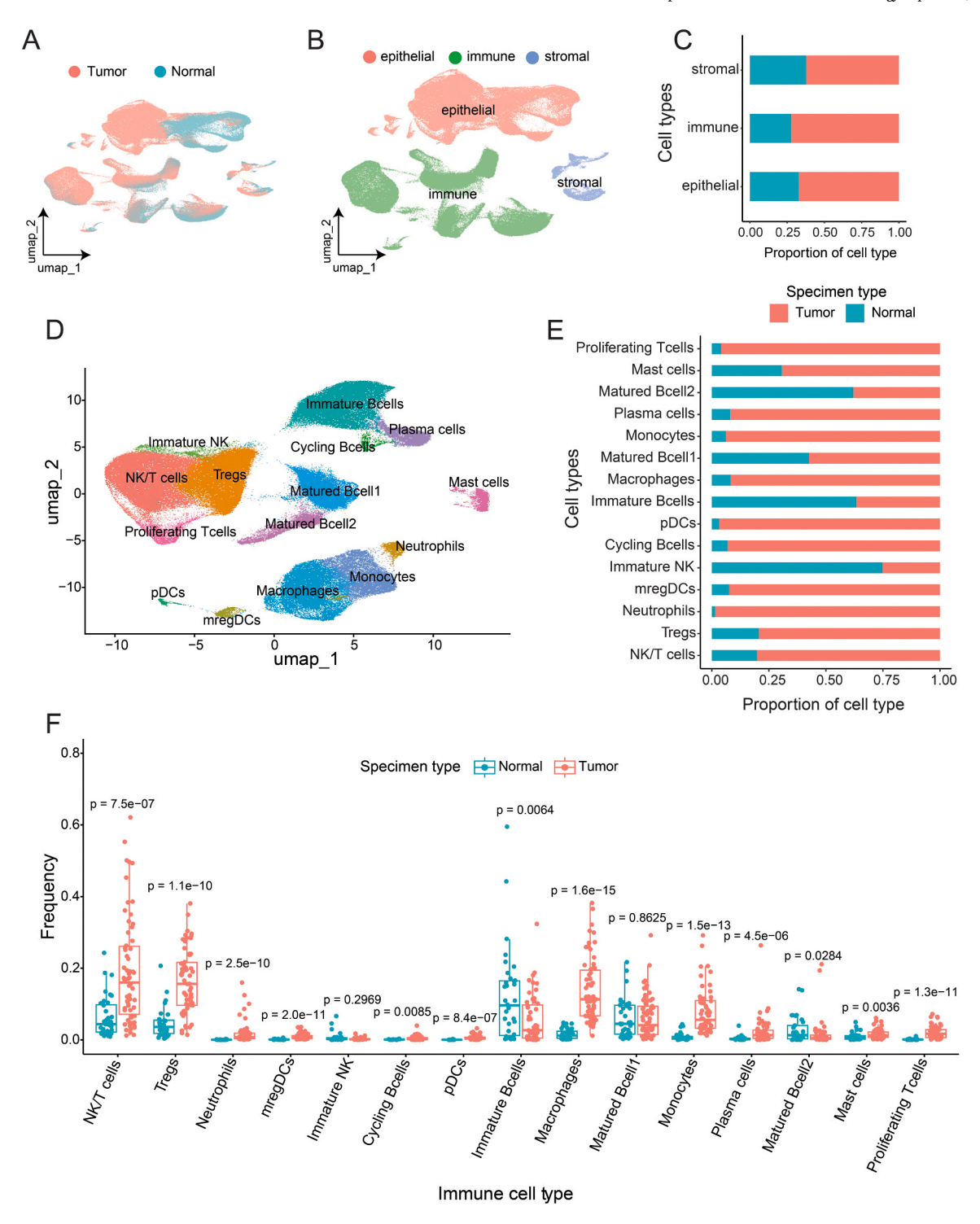


Fig. 1. Single-cell transcriptome profile of human colon cancer TME. A, UMAP plot showing the clustering of 370,114 high quality single-cells excavated from human colon tissues and their adjacent normal tissues. B, UMAP plot displaying three major cell classes of immune and non-immune cells in the tumor microenvironment. C, The proportion of the three major cell classes of immune and non-immune cells in the tumor and normal tissues. D, 2D UMAP plot of immune cells. E, Bar graph showing the proportions of each immune cell types in the tumor and normal tissues. F, Statistical assessment of the differences in the proportion of each cell types. *P*-value < 0.05 indicate that the difference in the cell type's expression counts between the two normal and tumor tissues is statistically significant. *P*-values were calculated by Wilcoxon test (wilcox.test).

necessarily rule out its potential contribution to CRC progression as previously described [22].

The up- and downregulated *TNFAIP8L2* co-expressed transcriptomes between normal and tumor tissues (Dco-EGs) were categorized at different significant *p*-value thresholds to identify biomarkers with prognostic significance (Fig. 3E). At a stringent threshold of *p*-value

< 0.001, we identified key Dco-EG markers including *ZG16* and *OLR1* (Fig. 3E) which were differentially expressed in Group 1 (Fig. 3F) and in the three myeloid cell types (Fig. 3G). *ZG16* was higher in the normal tissues, but lower in the tumor tissues, while *OLR1* showed an opposite trend. These two genes deserve further studies due to their potential roles in tumor immunity [26,33,34].

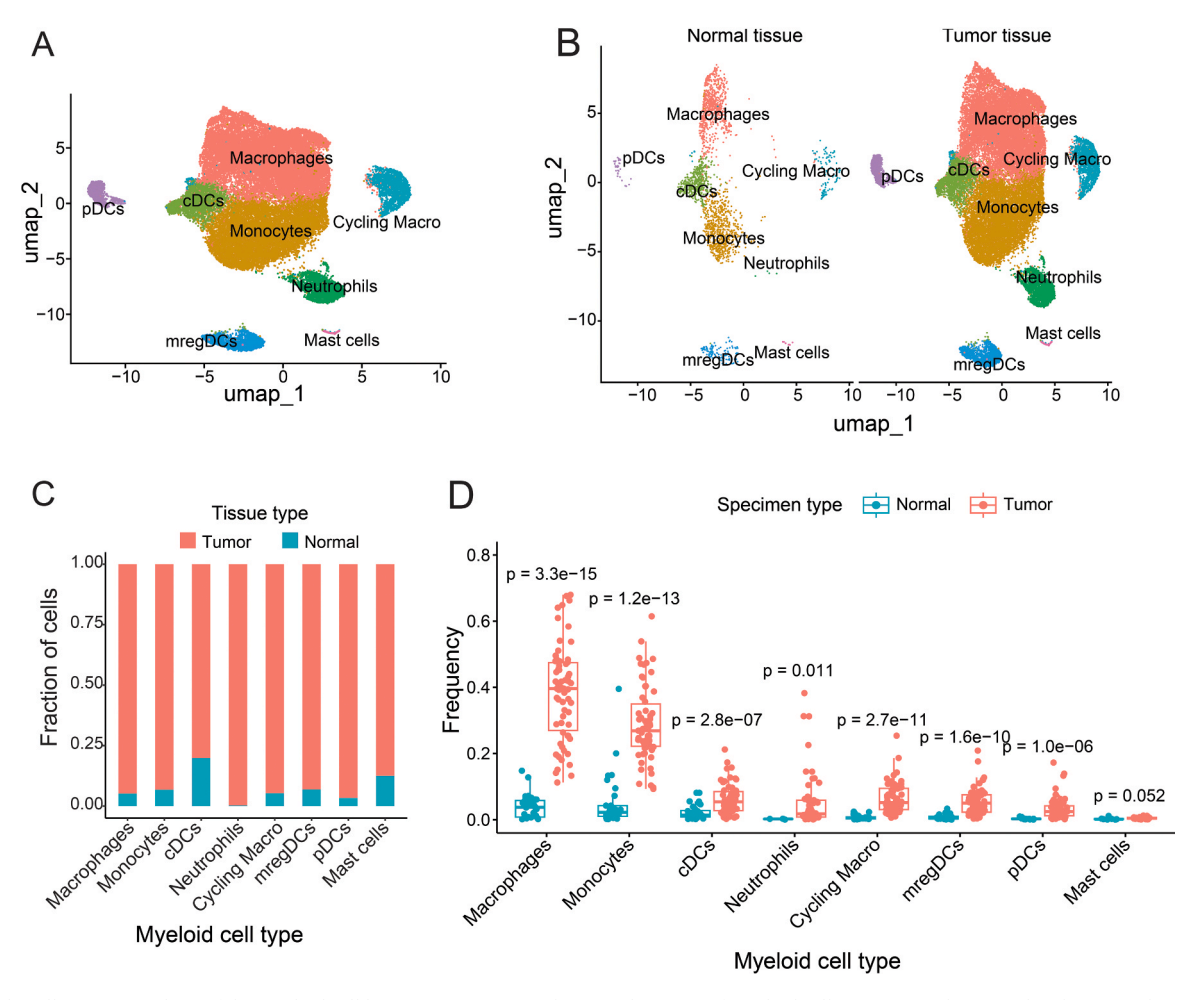


Fig. 2. Single-cell RNAseq analysis of the myeloid cell lineage. A-B, UMAPS showing clustering of myeloid cell types (A) in the normal and tumor colon tissues (B). C, Bar graph showing the proportion of normal and tumor tissue transcriptional expression counts of each myeloid cell type. D, The statistical assessment of the differences in the proportion of each myeloid cell type between normal and tumor tissues. The red and cyan solid circles are representative images of single-cells in either normal or tumor tissues. The differences with *p*-values < 0.05 estimated by Wilcoxon test (wilcox.test) were considered statistically significant.

Using TCGA bulk RNA data from a large cohort of CRC patients, we confirmed that the Dco-EG *OLR1* had a strong positive correlation with *TNFAIP8L2*, while the Dco-EG *ZG16* showed a weaker correlation (Fig. 4A-D, Figs. S3A-B). Prognostic assessment revealed that high *OLR1* expression was negatively associated with overall survival (OS) in patients (Fig. 4E), consistent with previous findings linking *OLR1* to high-grade malignancies and metastasis [26,34]. In contrast, high *ZG16* expression was positively correlated with OS of patients, consistent with reports that *ZG16* overexpression inhibits PD-1 expression and enhances anti-tumor immunity in CRC [26,34].

Functional enrichment analysis using the g:Profiler software (gprofiler2 package) [35] revealed that the Dco-EGs were enriched in gene ontological (GO) terms related to cell motility, leukocyte chemotaxis, and regulation of locomotion (Fig. 5A). Interestingly, they could also be linked to other pathways including signaling by interleukins, cytokine signaling in the immune system, and pathways related to rheumatoid arthritis. Upregulated Dco-EGs were associated with biological processes (BP) related to chemotaxis (Fig. 5B), indicating that these pathways were selectively activated to favor immune evasion mechanisms in colon cancer. In contrast, downregulated Dco-EGs were linked to antigen processing and presentation via MHC class II (Fig. 5C), suggesting their suppression to favor tumor progression.

Pathway RespOnsive GENes (PROGENy) analysis [36] of the three myeloid cell types "Macrophages," "Cycling Macro," and "cDCs," revealed differential regulation of signaling pathways. Macrophages upregulated p53-related pathways, while cycling macrophages and

dendritic cells exhibited significant upregulation of MAPK signaling pathways (Fig. S4). These findings suggest that *TNFAIP8L2* and its co-expressed genes, such as *OLR1* and *PD1* may collaborate to modulate immune escape through tumor suppressor genes such as *p53*.

2.4. Analyses of bulk RNA sequencing data confirmed TNFAIP8L2 coexpressed gene patterns in CRC

To further validate our findings, we analyzed TCGA bulk RNA expression data from a large cohort of CRC patients, focusing on the coexpression patterns of *TNFAIP8L2* with particular emphasis on *OLR1* and *ZG16*. Given the importance of immune checkpoints in cancer therapy, we also investigated the correlations between *TNFAIP8L2*, the Dco-EGs and several immune checkpoint markers.

Using the OncoDB database, we observed an insignificant negative correlation between *ZG16* and PD-1 (*CD274*) (Fig. S5A). Despite the lack of statistical insignificance, this negative relationship is consistent with previous studies showing that *ZG16* counteracts PD-1-mediated immune suppression [26]. In contrast, *OLR1* was not only positively correlated with *TNFAIP8L2* but also strongly correlated with PD-1 (Fig. S5B), suggesting a potential cooperative role in immune evasion.

TNFAIP8L2 exhibited a high degree of similarity with PD-1 (Fig. S5C), *CD28* (Fig. S5D) and *CD8A* (Fig. S5E). However, no significant correlation was observed between *TNFAIP8L2* and ICOSLG (Fig. S5F). Additionally, *TNFAIP8L2* showed a positive correlation with immunosuppressive CD4 +CD25 + Treg cell markers, such as FOXP3

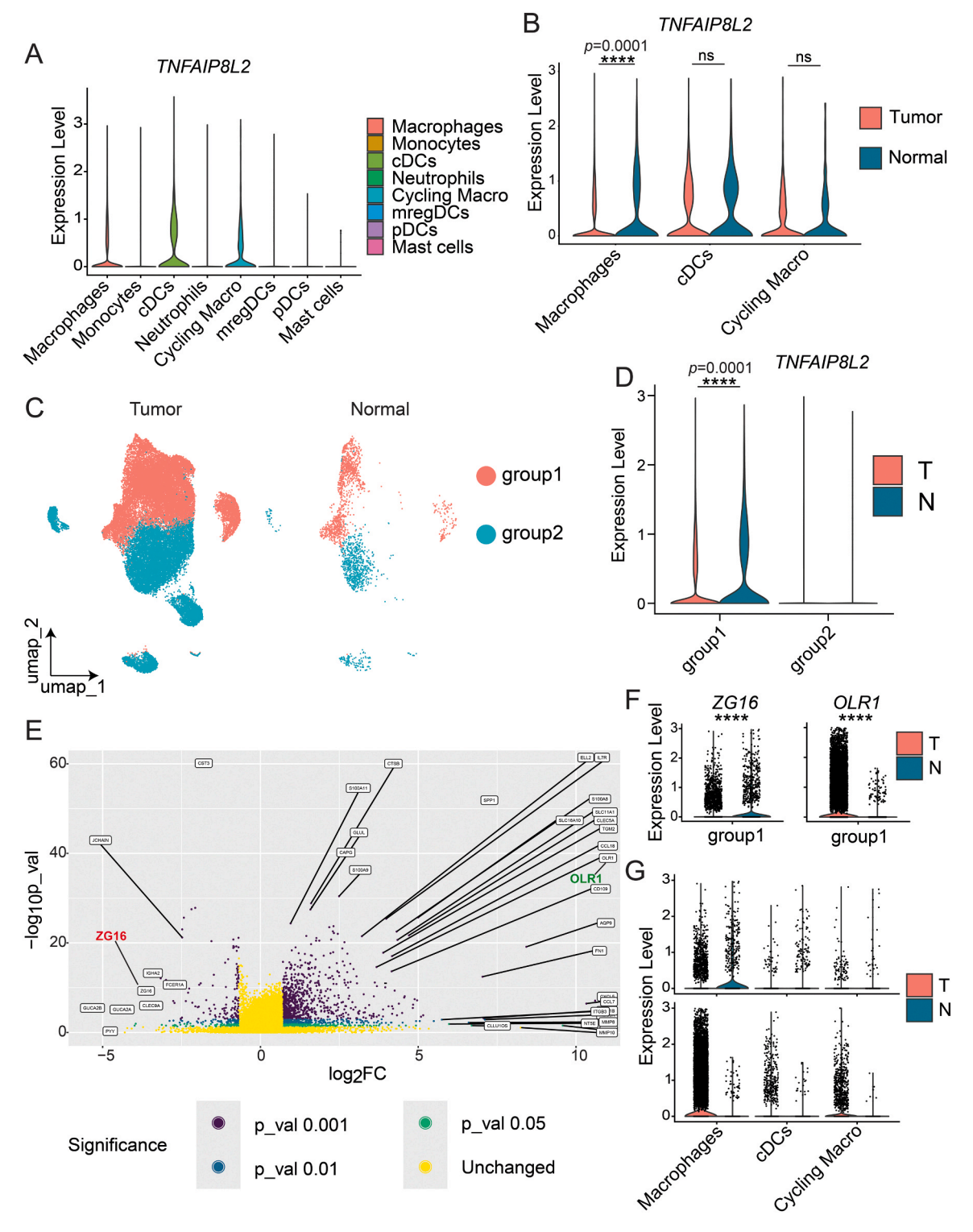


Fig. 3. Deconvolution analysis of *TNFAIP8L2* co-expression modules. A-B, violin plots illustrating the average expression levels of *TNFAIP8L2* in different myeloid cell types, which were high in macrophages, cDCs and cycling macrophages. C, Two groups of myeloid cell types annotated based on the expression of *TNFAIP8L2* with group 1 expressing *TNFAIP8L2* (total n cells = 19,501 with 1334 in normal tissues and 18,167 in tumor tissues) and group 2 not expressing *TNFAIP8L2* (total n cells = 15,428 with 876 and 14,552 in normal and tumor tissues, respectively). D, The average expression level of *TNFAIP8L2* is statistically different between normal and tumor tissues for group 1 cells. E, Volcano plot depicting *TNFAIP8L2* co-expressed genes in normal and tumor tissues. Three different *p*-value thresholds (*p*-values < 0.05, 0.01, and 0.001) were used to show the three different categories of co-expressed genes patterns, differentially expressed between normal and tumor tissues. F-G, violin plots depicting the average expressions of the selected DEGs (*ZG16* and *OLR1*) co-expressed with *TNFAIP8L2* in 19,501 group 1 cells (F) or among the three myeloid cell types, respectively (G). N, normal tissues; T, tumor tissues. Student t-test was used to analyze the difference in the gene expression levels in B, D, F and G.

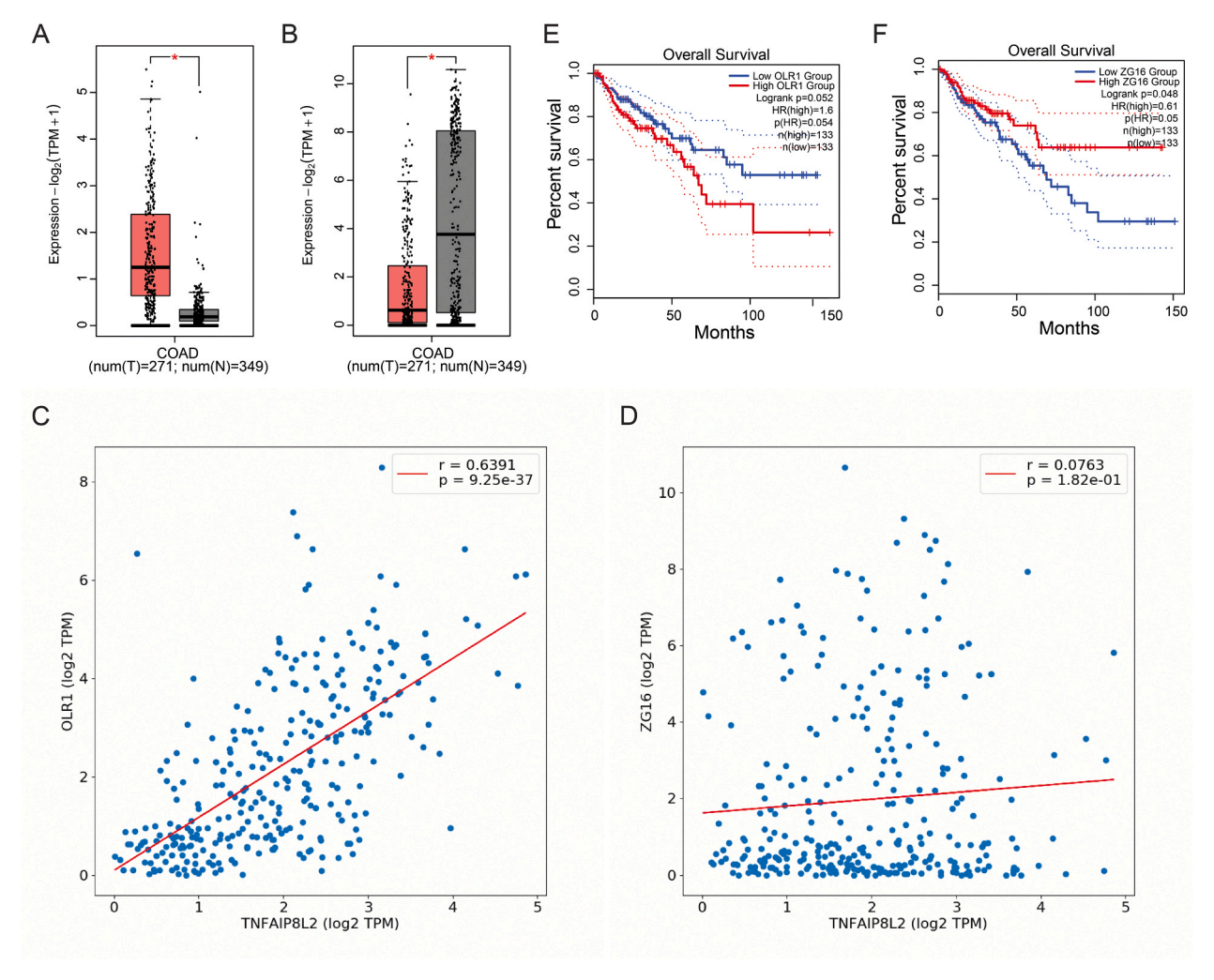


Fig. 4. Correlation and prognostic analysis of the selected co-expressions. A-B, Boxplots for the bulk RNA expression data of the selected *TNFAIP8L2* differentially co-expressed genes *OLR1* (A) and *ZG16* (B). C-D, Scatter plots showing the correlation between the selected Dco-EGs and *TNFAIP8L2* computed by OncoDB for *TNFAIP8L2* vs *OLR1* (C), and *TNFAIP8L2* versus *ZG16* (D). At an *r* value > 50 and a *p*-score < 0.05, the two genes were considered positively correlated significantly. E-F, Kaplan-Meier plots elaborating the extent of the overall survival of patients at high or low expressions of the tested genes *OLR1* (E) and *ZG16* (F).

(r = 0.724, p = 2.47 \times 10^-51) and *CTLA4* (r = 0.625, p = 9.05 \times 10^-35) (Figs. S5G and H). This finding suggests a potential cooperative relationship between *TNFAIP8L2* and Treg cells in mediating immunosuppression within the CRC TME by promoting the stability or functional activity of Tregs [30].

Our findings suggest a potential new immune evasion strategy in colon cancer, where the *TNFAIP8L2* and its co-expressed genes may synergize with immune checkpoints to exert a stronger collective effect on tumor progression than their individual contributions alone. This cooperative interaction warrants further investigation to uncover the underlying mechanisms driving CRC progression.

We assessed correlations between *TNFAIP8L2*, its co-expressed genes, and immune checkpoints using multiple databases (including GEPIA2 and OncoDB). The observed variations in correlation strengths (Fig. 4C-D, Supplementary Figs. S2A-B) may stem from differences in analytical methodologies and patient cohort characteristics.

3. Discussion

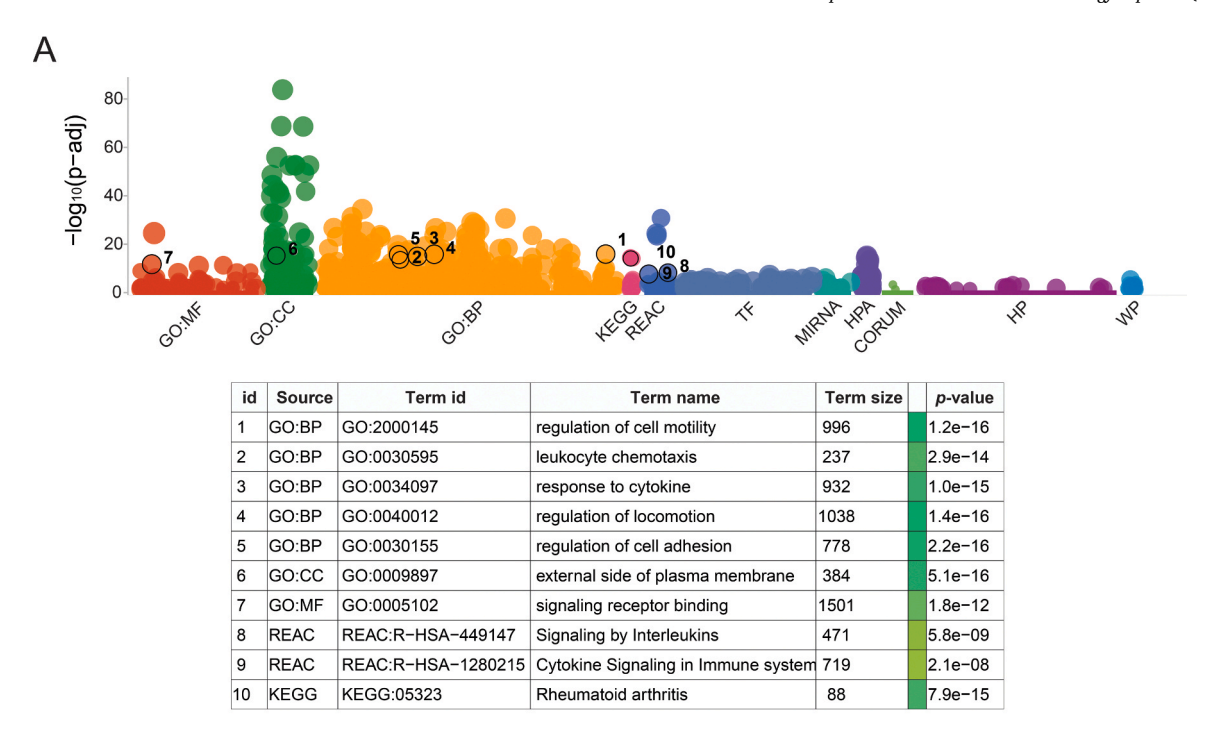
3.1. TNFAIP8L2 and human colorectal cancer

Colorectal cancer remains a significant global health burden [2,37], with immune evasion playing a central role in its progression and resistance to therapy [1]. Despite the clinical successes of immune

checkpoint therapies, their efficacy have still been limited particularly in microsatellite stable CRC patients [38]. This underscores the urgent need for identifying novel targets within the tumor microenvironment (TME) that can enhance anti-tumor immune responses, especially in combination with existing immunotherapeutic strategies.

In this study, we identified *TNFAIP8L2* as a potential crucial regulator of immune evasion in the CRC TME. As a member of the *TNFAIP8* family, *TNFAIP8L2* has been associated with immune homeostasis and cancer progression [19,20], but its role in human CRC has remained poorly understood. Our findings reveal a positive correlation between *TNFAIP8L2* expression and markers of regulatory T cells (Tregs) such as *FOXP3* and *CTLA4* - pivotal mediators of immune suppression in CRC [39–41]. We hypothesize that *TNFAIP8L2* cooperates with, or enhances, their activity to sustain an immunosuppressive tumor microenvironment.

Notably, it was first demonstrated previously that *TNFAIP8L2* (TIPE2) is highly expressed in CD4 +CD25 + Tregs and essential for their immunosuppressive capacity, as *TNFAIP8L2*-deficient Tregs exhibit impaired suppression of effector T-cell proliferation [30]. While their study did not examine molecular mechanisms linking *TNFAIP8L2* to specific Treg markers, we propose that *TNFAIP8L2* may potentiate *FOXP3* expression–a master regulator of Treg differentiation and suppressive function through: (1) Modulation of PI3K/Akt signaling, which directly controls *FOXP3* transcription via mTOR-dependent pathways



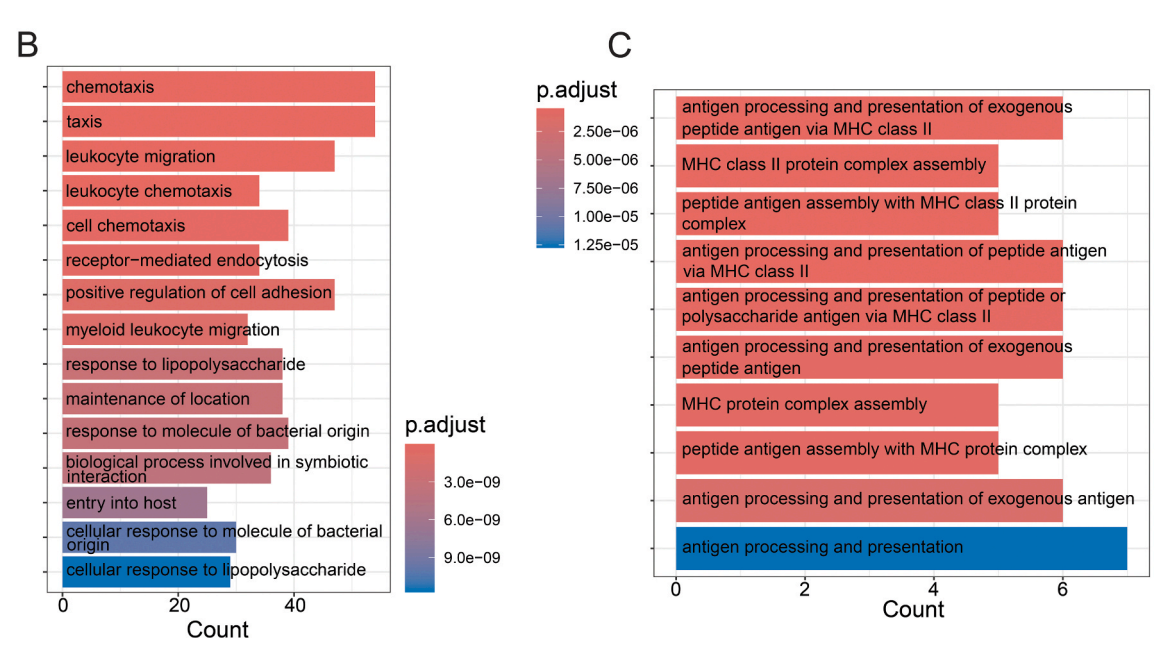


Fig. 5. Functional enrichment assessment of TNFAIP8L2 co-expression patterns. A, Manhattan dot plot describing the enriched biological processes associated with TNFAIP8L2 co-expression patterns. TNFAIP8L2 co-expressions referred to those co-expressed genes that were differentially expressed between normal and tumor tissues (i.e Dco-Egs) at p-value < 0.05, and $|\log 2FC| > 0.5$. Some of the selected GO terms, Reactome and KEGG pathways are indicated in the accompanied table, below plot A. B-C, Histogram plots depicting the specific pathways that might be associated with the upregulated (B) or downregulated Dco-Egs (C). P-adjusted values < 0.05 were considered to rule in the significantly enriched pathways, with the red to blue color at the scale bar indicating high to low degree of significance.

[42]; or (2) regulation of NF- κ B activity, which transactivates the *FOXP3* promoter [43,44]. Intriguingly, *TNFAIP8L2* has also been shown to impair autolysosome reformation by disrupting the *RAC1-MTORC1* axis [45], a process that may paradoxically stabilize Treg function in the TME by limiting excessive autophagy-driven turnover of immunosuppressive proteins.

While *TNFAIP8L2* enhances Treg activity in CRC, its role appears context-dependent. For instance, in dendritic cells (DCs) of the gut mucosa, *TNFAIP8L2* suppresses the induction of peripheral Tregs (pTregs) [46], suggesting tissue-specific regulation of immune tolerance. In contrast, within the CRC TME, *TNFAIP8L2* likely cooperates

with resident Tregs to sustain immunosuppression, potentially by synergizing with *CTLA4* to amplify checkpoint activity or by enhancing Treg survival via anti-apoptotic pathways (e.g., Bcl-2 upregulation).

This cooperative relationship extends the findings of Luan et al. (2011) by identifying potential mechanistic links between *TNFAIP8L2* and Treg molecular programs in CRC. The data align with the broader roles of PI3K/Akt signaling in cancer progression [47] and *TNFAIP8* family proteins in immune modulation, including their regulation of inflammatory pathways, T cell survival, and immunosuppressive niche formation [48–51]. *TNFAIP8L2* is thus positioned as a multifaceted regulator of immunosuppressive niches.

Our findings reveal that *TNFAIP8L2* is highly expressed in myeloid cell populations, particularly macrophages and dendritic cells, suggesting its involvement in shaping an immunosuppressive TME. Functional enrichment analyses indicated that genes co-expressed with *TNFAIP8L2* were enriched in critical pathways such as p53 signaling, leukocyte chemotaxis, and cytokine signaling, all of which are integral to immune regulation and tumor progression [36].

The differential regulation of these pathways among myeloid cell subsets specifically the enhanced expression of tumor-associated pathways like p53 and JAK-STAT in macrophages compared to conventional dendritic cells (cDCs) aligns with previous findings that myeloid cells exhibit a dual role in cancer, supporting or inhibiting anti-tumor immunity depending on their polarization and interactions within the TME [52].

3.2. The TNFAIP8L2-OLR1-PD-L1 axis: a potential therapeutic target

In this study, we identified significant co-expression patterns of *TNFAIP8L2* with pivotal immune regulators such as *OLR1*, *PDL1*, and *ZG16*. *OLR1*, known for its association with metastasis and poor prognosis [25], exhibited a positive correlation with *TNFAIP8L2*, suggesting a collaborative role in tumor progression. Conversely, *ZG16*, recognized for its anti-tumor properties [26], displayed an inverse relationship with *TNFAIP8L2*, indicating its potential to counteract the immune evasion facilitated by *TNFAIP8L2*. Together, these results underscore the intricate immune regulatory landscape in CRC, positioning *TNFAIP8L2* as a central node in a network of immune checkpoint interactions.

One striking revelation is the identification of the TNFAIP8L2-OLR1-PDL1 axis as a potential driver of immune evasion in CRC. The observed positive correlation among TNFAIP8L2, OLR1, and PDL1 suggests that these genes may function synergistically to suppress anti-tumor immunity. OLR1's role in promoting both metastasis and immune suppression may amplify the immunosuppressive effects conferred by TNFAIP8L2 and PDL1, particularly relevant for MSS CRC patients who often present resistance to therapies targeting PD-1 and PD-L1 [38]. Targeting this TNFAIP8L2-OLR1-PDL1 axis may therefore represent a novel therapeutic strategy for overcoming immune evasion in CRC. Approaches such as small-molecule inhibitors or gene-editing technologies like CRISPR-Cas9 could be employed to disrupt the function of TNFAIP8L2 or OLR1. Hence, combination therapies aimed at concurrently inhibiting TNFAIP8L2 and PDL1, OLR1 and PDL1, or TNFAIP8L2, OLR1, and PDL1 may enhance the effectiveness of existing immunotherapies, which might offer promising benefits for MSS CRC patients facing limited treatment efficacy with current immunotherapies [38].

3.3. ZG16 as a counterbalance to immune evasion

In contrast to the pro-tumor effects of *TNFAIP8L2* and *OLR1*, our findings highlight the protective role of *ZG16* in CRC. *ZG16*, identified as an anti-tumor gene, was found to be downregulated in tumor tissue and inversely correlated with *TNFAIP8L2* and *PDL1* expression. Patients exhibiting high *ZG16* expression demonstrated improved overall survival. The low or rather inverse correlations between *ZG16* and other markers suggests that *ZG16* may counteract immune evasion mechanisms driven by *TNFAIP8L2*, *OLR1*, and *PDL1*. These findings align with prior research indicating that *ZG16* inhibits PD-1 expression and enhances anti-tumor immunity in CRC [26,34].

Given its therapeutic potential, further exploration of ZG16 is warranted. Strategies aimed at upregulating ZG16 expression such as gene therapy or pharmacological interventions could offer a novel approach to enhance anti-tumor immunity in CRC. Additionally, ZG16 may serve as a biomarker to identify patients more likely to respond to immunotherapy, enabling personalized treatment strategies [26,34].

3.4. Limitations and future directions

While our study provides valuable insights into the potential role of *TNFAIP8L2* in CRC immune evasion, several limitations must be acknowledged. First, the functional mechanisms underlying *TNFAIP8L2*'s interactions with co-expressed genes such as *OLR1* and PD-L1 remain to be fully elucidated. Future studies should employ experimental approaches, such as gene knockout or knockdown models, to validate these interactions and explore the functional consequences.

Second, the clinical relevance of *TNFAIP8L2* expression and its coexpression patterns needs to be validated in larger patient cohorts, particularly across different CRC subtypes. This will help determine whether the *TNFAIP8L2-OLR1-PDL1* axis can serve as a reliable biomarker for predicting patient outcomes or guiding treatment decisions.

Finally, the integration of multi-omics data, including proteomics and epigenomics, could provide a more comprehensive understanding of *TNFAIP8L2-OLR1-PDL1*'s role in CRC progression and immune evasion. For example, proteomic analysis could reveal post-translational modifications of *TNFAIP8L2* that regulate its function, while epigenomic studies could identify upstream regulators of *TNFAIP8L2* expression.

3.5. Conclusion

Our study establishes *TNFAIP8L2* (TIPE2) as a critical immune checkpoint in myeloid cells, corroborating and expanding upon previous reports. We delineate the *TNFAIP8L2-OLR1-PDL1* axis as a therapeutically targetable pathway, particularly for microsatellite-stable (MSS) CRC patients who exhibit poor response to current immunotherapies. Additionally, *ZG16* known with its anti-tumor effects exhibits low correlation with *TNFAIP8L2*, suggesting a potential compensatory role in mitigating *TNFAIP8L2*-mediated immune suppression. Our comprehensive computational analyses unraveled key interactions within CRC's immune microenvironment, offering a translational roadmap for precision immunotherapy. Future investigations should focus on: (1) Functional validation of this axis in preclinical CRC models, (2) mechanistic studies to elucidate how *ZG16* counterbalances *TNFAIP8L2*, and (3) therapeutic development targeting the *TNFAIP8L2-OLR1-PD-L1* pathway to overcome immunotherapy resistance.

4. Materials and methods

4.1. Study design

The primary objective of this study was to identify potential mechanisms by which cancer cells evade anti-tumor immune responses, with a focus on the role of *TNFAIP8L2* in CRC. To achieve this, we employed computational methodologies to analyze publicly available single-cell and bulk RNA sequencing datasets focusing on CRC. Our analytical framework was designed to delineate the co-expression patterns and interrelationships of key cancer markers, with particular emphasis on *TNFAIP8L2*.

TNFAIP8L2, also known as TIPE2, is a member of the TIPE family of proteins, which also includes TIPE (TNFAIP8L), TIPE1 (TNFAIP8L1), and TIPE3 (TNFAIP8L3). TNFAIP8L2 was selected for detailed investigation due to its multifaceted biological significance, including its crucial roles in maintaining immune homeostasis, influencing cellular polarization, and orchestrating chemotaxis during tumorigenesis. Moreover, TNFAIP8L2 has been recognized as a marker for both tumor suppression and tumor propagation, underscoring its complex function within the oncogenic milieu.

4.2. Data acquisition

For this study, we curated single-cell RNA expression matrices from a cohort of 62 patients diagnosed with colon cancer [53], sourced from

the Gene Expression Omnibus (GEO) database of the National Center for Biotechnology Information (NCBI). Additionally, bulk RNA sequencing data from human colon cancer patients were obtained from The Cancer Genome Atlas (TCGA) via the OncoDB and GEPIA2 databases.

4.3. Single-cell RNA analysis and quality control

The gene expression matrix, which included integrated tumor and adjusted non-cancerous tissues from 62 patients [53], was processed in R software (versions 4.3.1, 4.3.2 and 4.4.0; R Core Team, 2023) (https:// www.R-project.org/) and the Seurat R package (version 5.0.1) [54]. To ensure the robustness of our clustering analysis, we employed stringent quality control measures to filter out low-quality cells and genes. Cells with fewer than 200 genes and genes expressed in fewer than three cells were systematically excluded. This step helped reduce noise and redundancy in the dataset, ensuring that only high-quality data were used for downstream clustering. Subsequently, Gene expression counts were normalized using the NormalizeData function with default parameters. Next, we identified the highly variable genes using the Find-VariableFeature function in Seurat, which selects genes that exhibit the most significant variation across cells. By focusing on these highly variable genes, we minimized the impact of redundant genes with overlapping expression patterns, thereby improving the resolution and biological relevance of the clustering results. To streamline the dataset and mitigate complexity, gene counts were scaled with ScaleData.

4.4. Dimensionality reduction and clustering

Dimensionality reduction was performed using principal component analysis (PCA), a widely used technique for reducing the complexity of high-dimensional scRNA-seq data. The number of principal components (PCs) to retain was determined using the ElbowPlot method, which identifies the inflection point where the explained variance begins to plateau. In our analysis, the top 20 PCs were selected as they captured the majority of the variance in the dataset while minimizing noise (Fig. S7). The use of PCA further reduced redundancy by summarizing the shared variation among genes, ensuring that the clustering algorithm focused on the most biologically meaningful signals. This approach ensures consistency across different settings of clustering outcomes.

Clustering was performed using the 'FindNeighbors' and 'FindClusters' functions, with the Louvain algorithm optimizing modularity. The resulting clusters were visualized using UMAP, a nonlinear dimensionality reduction technique that preserves both local and global structures in the data. This approach also allows to minimize the impact of redundancy on clustering outcomes and therefore the clusters we identified were biologically meaningful. The clusters were then annotated to their respective cell types based on canonical markers as described [54].

4.5. Co-expression analysis and functional enrichment

To unravel the co-expression patterns of *TNFAIP8L2*, we performed a series of analyses focusing on myeloid cell populations. First, the VlnPlot function in R was used to visualize myeloid cell subtypes expressing *TNFAIP8L2*. Cells expressing *TNFAIP8L2* were categorized as Group 1, while those without *TNFAIP8L2* expression were designated as Group 2. Genes expressed in Group 1 cells were labeled as *TNFAIP8L2* co-expressed genes, as they were co-expressed within the same cells. It should be noted that "self-interactions", defined as interactions between two or more copies of the protein that can interact with each other expressed by one gene, were explicitly excluded from the co-expression analysis since we focused on genes without multiple copies (see Quality Control) and that the results explicitly reflected genuine connections between *TNFAIP8L2* and other genes.

Comparative transcriptomic analysis between TNFAIP8L2-

expressing cells in normal and tumor tissues was performed using the FindMarkers function in Seurat with default settings to identify differentially co-expressed genes (Dco-EGs). Differential gene expression was visualized using volcano plots, and the identified Dco-EGs were evaluated for their associations with diagnostic, prognostic, and clinical parameters using large cohorts of CRC patients from TCGA.

Prognostic assessments were conducted using univariate Cox regression models and Kaplan-Meier survival curves to evaluate overall survival outcomes. The selected prognostic Dco-EGs along with *TNFAIP8L2* were analyzed for correlations with well-known immune checkpoints using the OncoDB [55] and GEPIA2 databases [56].

Functional enrichment analysis of the Dco-EGs was performed using the g:Profiler (gprofiler2 package) [35], which identified enriched GO terms, Reactome pathways, and Kyoto Encyclopedia of Genes and Genomes (KEGG) pathways. Significantly enriched terms and pathways were identified using a Bonferroni-corrected p-value threshold of < 0.05. Additionally, the cell types within Group 1 (TNFAIP8L2-expressing cells) were analyzed for their association with cancer-related regulatory pathways using the PROGENy tool [36].

4.6. Statistical analyses

Statistical analyses were performed to elucidate the patterns of *TNFAIP8L2* co-expression within single-cell gene expression data. The Seurat package (version 5.0.1) in R was used for clustering and visualization analyses. The differentially expressed genes were statistically tested using the MAST statistical test, and p-values were adjusted for multiple testing using the Bonferroni correction. The differences in the proportion of cells between normal and tumor tissues were evaluated using the Wilcoxon test (wilcox.test), while student *t*-test (t.test) was used to analyze the differences in the gene expression levels between normal and tumor tissues in Fig. 3B, D, F and G. Overall survival was calculated by means of the Kaplan–Meier method.

Author contributions

Y.H.C. and D.H.M. conceived and designed the study. D.H.M. analyzed the data and performed statistical analyses. D.H.M. interpreted data and drafted the manuscript. Y.H.C., T-H.W., H.X., O.W.S., I.A.B., Y. K., L. D., S. L., and P.L. revised the manuscript. All authors have reviewed and approved the final manuscript.

CRediT authorship contribution statement

Samuel Oluwarotimi Williams: Writing – review & editing, Visualization, Conceptualization. Babarinde Isaac A.: Writing – review & editing, Visualization, Methodology. Kong Yi: Writing – review & editing. Lang Shuyao: Writing – review & editing. Li Ping: Writing – review & editing. Mauki David H.: Writing – review & editing, Writing – original draft, Visualization, Methodology, Investigation, Formal analysis, Data curation. Chen Youhai: Writing – review & editing, Visualization, Supervision, Resources, Project administration, Funding acquisition, Conceptualization. Xia Houjun: Writing – review & editing, Visualization.

Ethics approval and consent to participate

This study did not require ethical approval as it used published datasets.

Funding

This work was supported by the National Natural Science Foundation of China (82250710172), Shenzhen Medical Research Fund (B2301006), the National Key R&D Program of China (2022YFA0912400), National Natural Science Foundation of China

(32130040), Shenzhen Science and Technology Program (JCYJ20220818100806015), and Shenzhen Medical Research Fund (B2404003).

Declaration of Competing Interest

Y.H.C. is a member of the boards of Amshenn and Binde Inc. The other authors have no conflicts of interest to declare.

Acknowledgment

The results of this study are, in part, based on data generated by TCGA Research Network: https://www.cancer.gov/tcga and from GEO repositories.

Appendix A. Supporting information

Supplementary data associated with this article can be found in the online version at doi:10.1016/j.csbr.2025.100041.

Data availability

The colorectal cancer single-cell RNA sequences underpinning this study were sourced from the GEO database with the accession code GSE178341. Additional data, particularly bulk RNA sequencing datasets supporting the conclusions drawn in this research article, are accessible via the OncoDB and GEPIA2 databases.

References

- [1] Brenner H, Kloor M, Pox CP. Colorectal cancer. Lancet 2014;383(9927):1490-502.
- [2] Ferlay J, et al. Estimates of worldwide burden of cancer in 2008: GLOBOCAN 2008. Int J Cancer 2010;127(12):2893–917.
- [3] Siegel R, Naishadham D, Jemal A. Cancer statistics, 2013. CA Cancer J Clin 2013; 63(1):11–30.
- [4] De Stefano A, Carlomagno C. Beyond KRAS: predictive factors of the efficacy of anti-EGFR monoclonal antibodies in the treatment of metastatic colorectal cancer. World J Gastroenterol 2014;20(29):9732–43.
- [5] Brabletz T, et al. Variable beta-catenin expression in colorectal cancers indicates tumor progression driven by the tumor environment. Proc Natl Acad Sci USA 2001; 98(18):10356–61.
- [6] Hanahan D, Weinberg RA. Hallmarks of cancer: the next generation. Cell 2011;144 (5):646–74.
- [7] Hanahan D, Coussens LM. Accessories to the crime: functions of cells recruited to the tumor microenvironment. Cancer Cell 2012;21(3):309–22.
- [8] Freeman GJ, et al. Engagement of the PD-1 immunoinhibitory receptor by a novel B7 family member leads to negative regulation of lymphocyte activation. J Exp Med 2000;192(7):1027–34.
- [9] Dong H, et al. Tumor-associated B7-H1 promotes T-cell apoptosis: a potential mechanism of immune evasion. Nat Med 2002;8(8):793–800.
- [10] Pardoll DM. The blockade of immune checkpoints in cancer immunotherapy. Nat Rev Cancer 2012;12(4):252–64.
- [11] Sharma P, Allison JP. The future of immune checkpoint therapy. Science 2015;348 (6230):56–61.
- [12] Grant MJ, Herbst RS, Goldberg SB. Selecting the optimal immunotherapy regimen in driver-negative metastatic NSCLC. Nat Rev Clin Oncol 2021;18(10):625-44.
 [13] Wu M, et al. Improvement of the anticancer efficacy of PD-1/PD-L1 blockade via
- combination therapy and PD-L1 regulation. J Hematol Oncol 2022;15(1):24.
- [14] Postow MA, Callahan MK, Wolchok JD. Immune checkpoint blockade in cancer therapy. J Clin Oncol 2015;33(17):1974–82.
- [15] Yang W, et al. Immune checkpoint blockade in the treatment of malignant tumor: current statue and future strategies. Cancer Cell Int 2021;21(1):589.
- [16] Hodi FS, et al. Improved survival with ipilimumab in patients with metastatic melanoma. N Engl J Med 2010;363(8):711–23.
- [17] Le DT, et al. PD-1 blockade in tumors with mismatch-repair deficiency. N Engl J Med 2015;372(26):2509–20.
- [18] Boland CR, Goel A. Microsatellite instability in colorectal cancer. Gastroenterology 2010;138(6):2073–2087.e3.
- [19] Sun H, et al. TIPE2, a negative regulator of innate and adaptive immunity that maintains immune homeostasis. Cell 2008;133(3):415–26.
- [20] Bi J, et al. TIPE2 is a checkpoint of natural killer cell maturation and antitumor immunity. Sci Adv 2021;7(38):eabi6515.
- [21] Bai KH, et al. Comprehensive analysis of tumor necrosis factor-α-inducible protein 8-like 2 (TIPE2): A potential novel pan-cancer immune checkpoint. Comput Struct Biotechnol J 2022;20:5226–34.

- [22] Li Y, et al. The overexpression of Tipe2 in CRC cells suppresses survival while endogenous Tipe2 accelerates AOM/DSS induced-tumor initiation. Cell Death Dis 2021;12(11):1001.
- [23] Fayngerts SA, et al. Direction of leukocyte polarization and migration by the phosphoinositide-transfer protein TIPE2. Nat Immunol 2017;18(12):1353–60.
- [24] Wang L, et al. TIPE-2 suppresses growth and aggressiveness of hepatocellular carcinoma cells through downregulation of the phosphoinositide 3-kinase/AKT signaling pathway. Mol Med Rep 2018;17(5):7017–26.
- [25] Yang G, et al. OLR1 promotes pancreatic cancer metastasis via increased c-Myc expression and transcription of HMGA2. Mol Cancer Res 2020;18(5):685–97.
- [26] Meng H, et al. ZG16 regulates PD-L1 expression and promotes local immunity in colon cancer. Transl Oncol 2021;14(2):101003.
- [27] Wang H, et al. Targeting p53 pathways: mechanisms, structures, and advances in therapy. Signal Transduct Target Ther 2023;8(1):92.
- [28] Ozga AJ, Chow MT, Luster AD. Chemokines and the immune response to cancer. Immunity 2021;54(5):859–74.
- [29] Lee M, Rhee I. Cytokine signaling in tumor progression. Immune Netw 2017;17(4): 214–27.
- [30] Luan YY, et al. Expression of tumor necrosis factor-α induced protein 8 like-2 contributes to the immunosuppressive property of CD4(+)CD25(+) regulatory T cells in mice. Mol Immunol 2011;49(1-2):219–26.
- [31] Yiu AJ, Yiu CY. Biomarkers in colorectal cancer. Anticancer Res 2016;36(3): 1093–102.
- [32] Bischoff P, et al. Single-cell RNA sequencing reveals distinct tumor microenvironmental patterns in lung adenocarcinoma. Oncogene 2021;40(50): 6748–58
- [33] Murdocca M, et al. LOX-1 and cancer: an indissoluble liaison. Cancer Gene Ther 2021;28(10-11):1088–98.
- [34] Meng H, et al. Loss of ZG16 is associated with molecular and clinicopathological phenotypes of colorectal cancer. BMC Cancer 2018;18(1):433.
- [35] Kolberg L, et al. gprofiler2 an R package for gene list functional enrichment analysis and namespace conversion toolset g:Profiler. F1000Res 2020;9.
- [36] Schubert M, et al. Perturbation-response genes reveal signaling footprints in cancer gene expression. Nat Commun 2018;9(1):20.
- [37] Sung H, et al. Global Cancer Statistics 2020: GLOBOCAN estimates of incidence and mortality Worldwide for 36 Cancers in 185 Countries. CA Cancer J Clin 2021; 71(3):209–49.
- [38] Sahin IH, et al. Immunotherapy for microsatellite stable colorectal cancers: challenges and novel therapeutic avenues. Am Soc Clin Oncol Educ Book 2022; (42):242–53.
- [39] Cui K, et al. Identification of an immune overdrive high-risk subpopulation with aberrant expression of FOXP3 and CTLA4 in colorectal cancer. Oncogene 2021;40 (11):2130-45.
- [40] Wing K, et al. CTLA-4 control over Foxp3+ regulatory T cell function. Science 2008;322(5899):271-5.
- [41] Qiu Y, et al. FOXP3+ regulatory T cells and the immune escape in solid tumours. Front Immunol 2022;13:982986.
- [42] Sauer S, et al. T cell receptor signaling controls Foxp3 expression via PI3K, Akt, and mTOR. Proc Natl Acad Sci USA 2008;105(22):7797–802.
 [43] Eckerstorfer P, et al. Proximal human FOXP3 promoter transactivated by NF-
- [43] Eckerstorfer P, et al. Proximal human FOXP3 promoter transactivated by NF-kappaB and negatively controlled by feedback loop and SP3. Mol Immunol 2010; 47(11-12):2094–102.
- [44] Jana S, et al. The role of NF-kappaB and Smad3 in TGF-beta-mediated Foxp3 expression. Eur J Immunol 2009;39(9):2571–83.
- [45] Li W, et al. TNFAIP8L2/TIPE2 impairs autolysosome reformation via modulating the RAC1-MTORC1 axis. Autophagy 2021;17(6):1410–25.
- [46] Liu R, et al. TIPE2 in dendritic cells inhibits the induction of pTregs in the gut mucosa. Biochem Biophys Res Commun 2019;509(4):911–7.
- [47] He Y, et al. Targeting PI3K/Akt signal transduction for cancer therapy. Signal Transduct Target Ther 2021;6(1):425.
- [48] Lou Y, Liu S. The TIPE (TNFAIP8) family in inflammation, immunity, and cancer. Mol Immunol 2011;49(1-2):4-7.
- [49] Goldsmith JR, Chen YH. Regulation of inflammation and tumorigenesis by the TIPE family of phospholipid transfer proteins. Cell Mol Immunol 2017;14(12): 1026.
- [50] Lou Y, et al. TNFAIP8 protein functions as a tumor suppressor in inflammation-associated colorectal tumorigenesis. Cell Death Dis 2022;13(4):311.
- [51] Cheng X, et al. TNFAIP8 modulates the survival and immune activity of Th17 cells via p53/ p21/ MDM2 pathway after acute insult. Cytokine X 2022;4(1):100062.
- [52] Chang RB, Beatty GL. The interplay between innate and adaptive immunity in cancer shapes the productivity of cancer immunosurveillance. J Leukoc Biol 2020; 108(1):363–76.
- [53] Pelka K, et al. Spatially organized multicellular immune hubs in human colorectal cancer. Cell 2021;184(18):4734–52. .e20.
- [54] Hao Y, et al. Integrated analysis of multimodal single-cell data. Cell 2021;184(13): 3573–87. e29.
- [55] Tang G, Cho M, Wang X. OncoDB: an interactive online database for analysis of gene expression and viral infection in cancer. Nucleic Acids Res 2022;50(D1). p. D1334-d1339.
- [56] Tang Z, et al. GEPIA2: an enhanced web server for large-scale expression profiling and interactive analysis. Nucleic Acids Res 2019;47(W1). p. W556-w560.